



Cite this: DOI: 10.1039/c5nj02199e

Implications of flexible spacer rotational processes on the liquid crystal behavior of 4,5-dihydroisoxazole benzoate dimers†

Aline Tavares,^{*a} Josene M. Toldo,^a Guilherme D. Vilela,^a Paulo F. B. Gonçalves,^a Ivan H. Bechtold,^b Stuart P. Kitney,^c Stephen M. Kelly^d and Aloir A. Merlo^{*a}

The synthesis of some novel non-symmetric liquid crystal dimers, {3-[4-(octyloxyphenyl)]-4,5-dihydroisoxazol-5-yl}alkyl 4-(decyloxy)benzoates (**5a–d**) and 4-{3-[4-(octyloxyphenyl)]-4,5-dihydroisoxazol-5-yl}alkyl 4-{[6-(octyloxy)naphthalen-2-yl]ethynyl}benzoate (**9a–d**), are reported. The liquid-crystalline properties, theoretical calculations based on the conformational aspects of the flexible alkyl spacer and X-ray experiments are discussed. The syntheses of the key intermediates, 2-{3-[4-(octyloxy)phenyl]-4,5-dihydroisoxazol-5-yl}alkanol (**3a–d**), presenting the flexible alkyl spacer were achieved through [3+2] cycloaddition reactions between nitrile oxides, which were generated *in situ* by oxidation of the respective aromatic oximes, and dipolarophile alkenols (CH₂=CH(CH₂)_nOH, *n* = 1, 2, 3, and 4). The benzoates **5a–d** were synthesized through esterification of **3a–d** and *p*-*n*-decyloxybenzoic acid (**4**). The esters **9a–d** were synthesized through derivatization of isoxazolines **3a–d** into 4-{3-[4-(octyloxyphenyl)]-4,5-dihydroisoxazol-5-yl}alkyl 4-bromobenzoate (**7a–d**) followed by a Sonogashira reaction with 2-ethynyl-6-octyloxynaphthalene (**8**). **5a** and **5b** showed a monotropic smectic C phase. **9a/c** displayed an enantiotropic nematic (N) mesophase, whereas **9b/d** showed a monotropic nematic mesophase. No mesophase was observed for **7a–d**. An odd–even effect was observed for **5a–d** and **9a–d** associated with the crystal to isotropic phase transition and crystal to nematic phase, respectively, as the length of the spacer was increased from 1 to 4 carbon atoms. The transitional properties were higher for odd-numbered members (*n* = 1 and 3) for all of the series studied. The X-ray data of compounds **5a** and **5b** are in agreement with polarizing optical microscopy observations with the assignment of an SmC mesophase. Density functional theory calculations using the B3LYP hybrid functional with the level 6-311G(d,p) basis set were performed for molecules **5a–d** to correlate the conformation of the flexible spacer and the transitional properties. The conformational analysis showed that the most stable conformation for **5a–d** is one where all of the carbon atoms of the flexible spacer are orientated at 180° (*antiperiplanar* orientation) except for **5a** because the spacer is too short. The odd-numbered members have a more bent shape and are less elongated molecules than the even-numbered members. Thus, mesomorphic behavior is dictated by the conformational constraint imposed by the flexible spacer on the mesogenic groups.

Received (in Montpellier, France)
18th August 2015,
Accepted 16th October 2015

DOI: 10.1039/c5nj02199e

www.rsc.org/njc

Introduction

Liquid crystal oligomers (LCOs) are a special class of soft materials formed of two or more anisotropic-shaped cores connected by flexible spacers, normally alkyl chains.¹ The core

is usually a mesogenic group and the simplest LCOs are termed dimers which have just two mesogenic units linked chemically to a single methylene chain.² The first reports about liquid crystal dimers were by Vorländer³ at the beginning of the 1920s and by Rault⁴ some years later. However, these important reports appear to have been a forgotten past until the early 1980s, when they were rediscovered again and gained new interest.⁵ The vast majority of LCOs are composed of two symmetric rod-like mesogenic units,⁶ whereas their non-symmetrical analogues⁷ have two different mesogenic groups connected by a flexible alkyl chain and less frequently by oligo(ethyleneoxide),⁸ oligo(siloxane)⁹ and sulfur–sulfur links¹⁰ in the chain. In this context, the length and parity of the flexible spacer are important parameters that have

^a Institute of Chemistry, UFRGS, Porto Alegre, RS, Brazil.
E-mail: aloir.merlo@ufrgs.br

^b Department of Physics, UFSC, Florianópolis, Brazil

^c Polar OLED, University of Hull, Hull, England, UK

^d Department of Chemistry, University of Hull, Hull, UK

† Electronic supplementary information (ESI) available: Experimental procedure, ¹H and ¹³C NMR spectrum and spectroscopic data final compounds, modeling pictures of the rotamers. See DOI: 10.1039/c5nj02199e

a great influence on the transitional properties.¹¹ Dimers and higher oligomers, such as trimers^{12–14} and tetramers,^{15,16} have a special level of attention due to their ability to act as model compounds for semi-flexible main-chain liquid crystal polymers.^{17,18} Also, from the academic point of view these oligomers are interesting because they behave differently to conventional liquid crystals of low molar mass.^{19,20}

Mostly, LCOs have an aryl group as the mesogenic unit and a few examples of LCOs incorporating 5- and 6-membered rings such as 1,3,4-oxadiazoles and pyridyl-based dimers respectively, have also been published, with their transitional properties having been investigated.^{21,22} Compounds containing a 4,5-dihydroisoxazole moiety have been prepared recently and the liquid crystalline behavior evaluated.²³ To the best of our knowledge, however, there have been no examples of non-symmetric 4,5-dihydroisoxazole-based liquid crystal dimers reported in the literature.

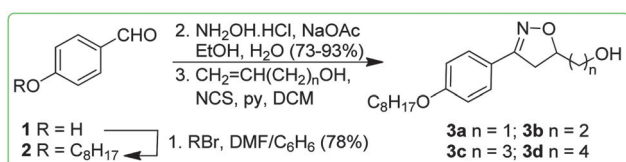
We have previously reported²⁴ the synthesis of liquid-crystalline 3,5-disubstituted isoxazolines, where the number of carbon atoms of the terminal aliphatic chains exerts a strong influence on the molecular shape and mesomorphic behavior. In this work, we report the synthesis and transitional properties of two new homologous series of non-symmetrical 3,5-disubstituted 4,5-dihydroisoxazole benzoate liquid crystal dimers with emphasis on the dependence of the liquid-crystalline transition temperatures on the number of methylene carbon atoms of the flexible spacer. Density functional theory (DFT) calculations combined with X-ray analysis provided supporting information in this study.

Results and discussion

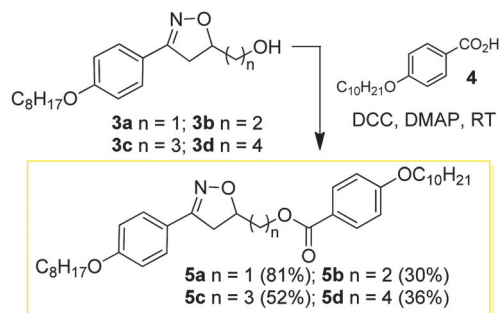
Synthesis and description of liquid-crystalline behavior

The synthetic route used for the preparation of the isoxazolines **3a–d** is shown in Scheme 1. We selected the aldehyde **2** as a precursor for the reactive aryl nitrile oxide.²⁵ Thus, the aldehyde **2** was synthesized through alkylation of 4-hydroxybenzaldehyde **1** with octylbromide in 78% yield. The isoxazolines were obtained by a [3+2] 1,3-dipolar cycloaddition²⁶ of nitrile oxide, formed by the *in situ* oxidation reaction of 4-octyloxybenzaldehyde oxime and four different dipolarophile alkenols – CH₂=CH(CH₂)_nOH, *n* = 1, 2, 3, and 4. The final key isoxazolines **3a–d** were obtained in low yields (33–36%).

The design and synthesis of the liquid crystals **5a–d** and **9a–d** was based on creating the structural characteristics necessary for the occurrence of a mesophase through a short and quick synthesis. Thus, the first homologous series **5a–d**, (see reaction Scheme 2) was prepared through the esterification of



Scheme 1 Synthetic route used to prepare compounds **3a–d**.



Scheme 2 Preparation of 3,5-disubstituted 4,5-dihydroisoxazole benzoate dimers **5a–d**.

compounds **3a–d** and 4-*n*-decyloxybenzoic acid **4** in the presence of DCC and catalytic amounts of DMAP in a THF solution at room temperature. The compounds **7a–d**, prepared from the esterification reaction between compounds **3a–d** and 4-bromobenzoic acid **6** in the presence of DCC and catalytic amounts of DMAP in THF, were precursors for the synthesis of the liquid-crystalline materials **9a–d**. The yields reported for the compounds **5a–d** and **7a–d** refer to the pure compounds after purification *via* recrystallization or column chromatography to remove the undesirable byproduct urea.

The compounds **9a–d** were prepared using a Sonogashira cross-coupling reaction between the intermediates **7a–d** and the terminal alkyne **8** in the presence of a palladium catalyst, *i.e.*, (PPh₃)₂PdCl₂, CuI, PPh₃ in NEt₃ (Chart 1).

The mesophase identification for the LC compounds **5a–d** as well as for **9a–d** was made using polarizing optical microscopy (POM). The smectic C mesophase (SmC) was assigned through the observation of a typical broken fan texture (at the top of Fig. 1(A) for **5a**) and a schlieren texture (at the bottom of Fig. 1(C) for **9b**). For compound **5b**, the mesophase SmC range was very narrow and it appears very quickly before the crystallization takes place [Fig. 1(B)]. The DSC traces for **5b** display a shoulder along a peak related to the transition temperature of the crystal phase to the isotropic phase. The SmC mesophase for **5c** and **5d** was detected and the texture persists for just a few seconds followed by fast crystallization. No POM images or

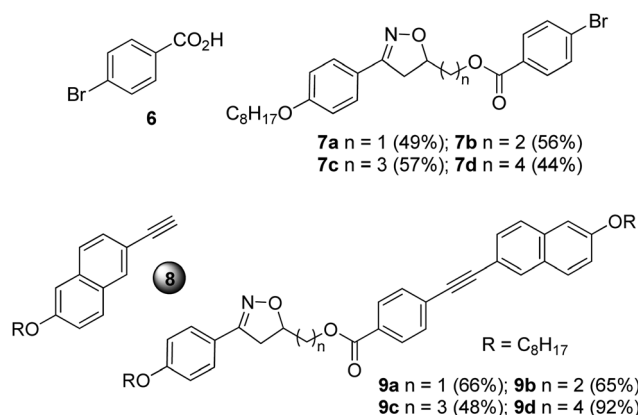


Chart 1 Intermediates and final compounds of the series **7a–d** and **9a–d**.

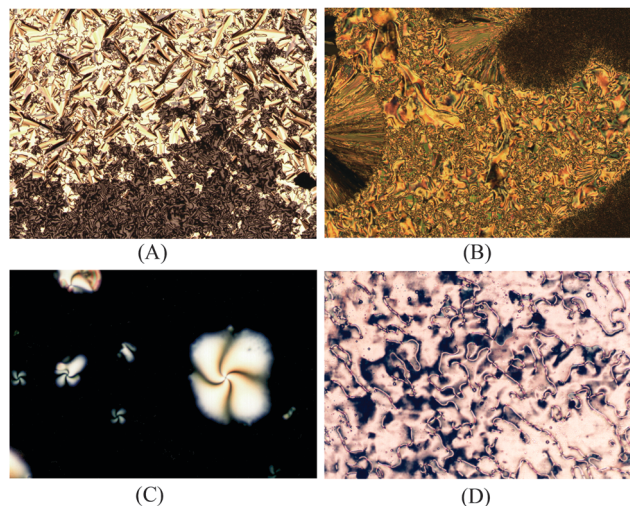


Fig. 1 Photomicrographs of the textures obtained from optical microscopy on cooling ($\times 10$) of: (A) the broken fan texture (at the top) and schlieren texture (at the bottom) of the SmC mesophase displayed by compound **5a** below 79 °C, (B) the coexistence of the broken fan texture of the SmC mesophase and crystal phase displayed by compound **5b** below 58 °C in fast cooling, (C) the schlieren texture of the nematic mesophase displayed by compound **9b** below 129 °C, (D) the thread-like texture of the nematic mesophase displayed by compound **9d** below 120 °C.

shoulders in the DSC traces for these compounds could be acquired. Identification of the nematic mesophase for compounds **9a–d** was made from the observation of the typical schlieren texture with two- and four-point brushes and a planar texture [Fig. 1(C) and (D)]. The low enthalpy values associated with the transition of the nematic mesophase to the isotropic state corroborate this assignment (see Table 1).

Compounds **5a–d** are composed of two terminal alkyl chains – eight carbon atoms on the isoxazoline side and ten carbon atoms

on the ester side. The number of carbon atoms in the flexible spacer was varied. So, compounds **5a–d** have $n = 1, 2, 3,$ and 4 in the flexible spacer, respectively.

The transition temperatures shown in Table 1 were obtained through a combination of POM and DSC analysis. Compounds **5a** and **5b**, upon a second cooling cycle, exhibit a monotropic phase with two exothermic peaks at 83 °C and 61 °C, respectively. These peaks were associated with the transition temperature when the samples enter the SmC mesophase from the isotropic state. Upon further cooling, **5a** and **5b** displayed a crystallization peak from the SmC mesophase, at 74 °C and 54 °C, respectively. For the higher homologues **5c** and **5d**, the DSC traces show only peaks related to the crystal phase to isotropic phase transition. However, samples of **5c** and **5d** when analyzed using POM upon fast cooling, displayed a monotropic SmC phase before recrystallization. For compounds that belong to the homologous series **9a–d** the terminal alkyl chain was fixed at eight carbon atoms (n -octyl). The variation in the flexible spacer was made in the same way as described for **5a–d**. According to the DSC data [Table 1, Fig. 1(C) and (D) and Fig. S31 (ESI†)], the **9a** and **9c** homologues of this series exhibit an enantiotropic nematic mesophase, while **9b** and **9d** display a monotropic nematic mesophase. When heated, the temperature range decreased by increasing the number of methylene units in the aliphatic chain, *e.g.*, for **9a** $\Delta T = 13$ °C and for **9c** $\Delta T = 9$ °C. For **9b** and **9d**, a monotropic nematic mesophase was observed which was more persistent for **9d**, whereas **9b** displayed a nematic mesophase for a few seconds through quick cooling from the isotropic state to under room temperature. Under this circumstance the nematic mesophase grew along with the crystal formation.

Compounds **9a–d** have a more pronounced rod-like or lath-like structure than compounds **5a–d** and **7a–d** and, consequently, they exhibit an enantiotropic mesophase at higher temperatures than compounds **5a–d**.

Table 1 Liquid-crystalline transition temperatures (°C),^a and enthalpy and entropy values (kcal mol⁻¹) for the homologous series **5a–d**, **7a–d**, and **9a–d**

Entry	Transition phase temperatures		ΔT , ^e °C	Enthalpy, ΔH		Entropy, $\Delta S/R$ ^g
	Heating	Cooling		Melt ^f	I/phase/Cr	
5a	Cr 103 I	I 83 SmC 74 Cr	9	17.9	I/3.1 SmC/10.4 Cr	24.0
5b	Cr 72 I	I 61 SmC 54 Cr	7	8.7	—	12.5
5c	Cr 85 I	I 66 Cr ^c	—	23.0	—	32.4
5d	Cr 68 I	I 57 Cr ^c	—	13.4	—	19.5
7a	Cr 115 I ^b	I 104 Cr	—	—	—	—
7b	Cr 90 I ^b	I 77 Cr	—	—	—	—
7c	Cr 99 I ^b	I 81 Cr	—	—	—	—
7d	Cr 73 I ^b	I 61 Cr	—	—	—	—
9a	Cr 150 N 163 I	I 162 N 136 Cr	13	13.0	I/0.4 N/13.2 Cr	15.4
9b	Cr 130 I	I N ^d 120 Cr	—	10.0	I/—/10.5 Cr	12.4
9c	Cr 136 N 145 I	I 144 N 126 Cr ₁ 116 Cr ₂	9	9.3	I/0.9 N/0.8 Cr ₁ 8.5 Cr ₂	11.5
9d	Cr 130 I	I 122 N 112 Cr	10	12.7	I/0.5 N/11.5 Cr	15.8

^a Onset temperatures (T_{onset}). Data obtained from DSC (2nd cycle) with a rate of heating and cooling of 10 °C min⁻¹; Cr = crystal phase, SmC = smectic C mesophase, N = nematic mesophase, and I = isotropic liquid. ^b Temperatures were obtained through optical microscopy. ^c SmC or ^d N mesophases were observed only on fast cooling – samples were exposed to room temperature. ^e Mesophase range upon cooling for compounds **5a–b** and **9d** and upon heating for **9a** and **9c**. For **9b** the temperature range was too small to be measured. ^f Enthalpy values (second cycle heating/cooling) obtained in the Cr–I transition for the series **5a–d** and the Cr–N transition for the series **9a–d**. ^g Values of melting entropy obtained in the Cr–I transition for the series **5a–d** and **9b/d** and Cr–N for **9a/c**. $R = 8.31 \text{ J K}^{-1} \text{ mol}^{-1}$.

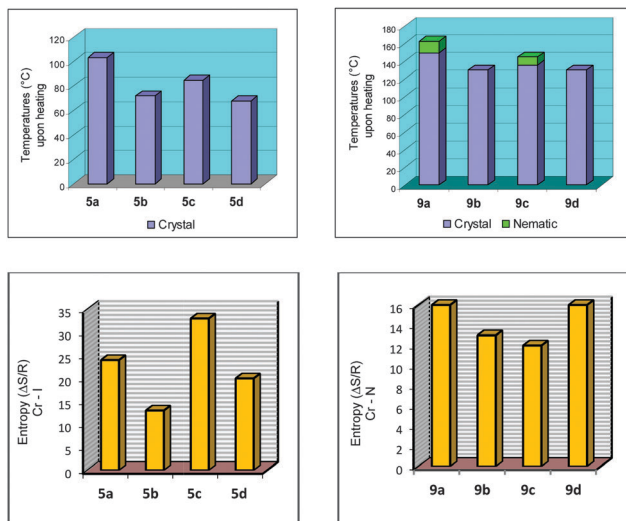


Fig. 2 Bar graphs for **5a–d** and **9a–d**. Plots of temperatures (°C) upon heating (top) and entropy values for Cr → I for **5a–b** and Cr → N for **9a–d** ($\Delta S/R$) (bottom).

The melting points for **5a–d**, **7a–d** and **9a–d** displayed an odd–even effect as the length and parity of the flexible spacer was varied. The values of the melting point alternate as the length of the flexible spacer chain increase with odd-numbered members exhibiting higher values. The alternation is attenuated by increasing the spacer length. Values of the entropy associated with the melting points of **5a–d** displayed the odd–even effect while those for **9a–d** did not follow the tendency observed for **5a–d**, probably due to the nature of the mesophase accompanying the crystal phase (Fig. 2). The melting processes followed the same tendency as noted for the melting points of the compounds.

For the homologous series **9a–d** the odd–even effect based on the mesomorphic behavior is also barely observed upon cooling the samples from the isotropic phase. A stable nematic mesophase was observed for **9a** and **9c**, however, for **9b** and **9d** the nematic mesophase was only visible during the cooling cycle. **9b** displayed the N mesophase upon cooling with a very short period of time [Fig. 1(C)]. Upon cooling, all samples showed a nematic mesophase. The correlation between the length and parity of the flexible spacer is not an easy task to achieve considering that upon heating **9b** and **9d** did not display mesomorphic behavior. The influence of the flexible spacer for compounds **9a–d** is more visible and more pronounced due to the more anisotropic shape of the molecules of this series than the series **5a–d**. The naphthyl group connected by triple bond to the benzoate moiety induces the formation of a stable mesophase when compared to the series **5a–d**. However, a conformational issue associated with the methylene chain flexible spacer alters the molecular packing in the mesophase, and consequently induces a dependence of the intermolecular interaction between the aromatic ring and the size of the flexible spacer. When we move along the carbon skeleton of the flexible spacer, the aromatic rings rotate around the last carbon bond to produce a set of distinct conformations for **9a/c** and **9b/d** (see the Theoretical calculations section). Obviously, the transitional

properties analysis in this article suffers a drawback because the nematic phase behavior is only stable for **9a** and **9c**. However, upon heating or cooling the melting points exhibit an even–odd effect as shown in Fig. 2 for the **5a–d** and **9a–d** series. The odd-numbered members have the highest values (**9a** and **9c**) and the even-numbered members have the lowest values (**9b** and **9d**). The odd-numbered members displayed higher values of melting point than the even-numbered members.

The dependence of the entropy changes associated with the nematic crystal–isotropic transition on the number of methylene units (n) present in the flexible spacer of non-dimeric LC **9a–d** does not follow a regular tendency due to the nature of the nematic phase observed in this series of liquid crystals (Fig. 2, bottom). Anyway, it is possible to state that the differences between odd and even membered dimers reflect, at least, the difference in their average molecular shapes, which are governed to a large extent by the parity of the flexible spacer.¹

Transitions from a more ordered mesophase to the isotropic state have higher entropy than transitions between a disordered phase to the isotropic state. Less ordered phases, such as the nematic phase, display lower entropy values and consequently, when they undergo a transition to the isotropic liquid state are less sensitive to structural parameters, such as variation in the flexible spacer, due to the absence of short- or long-positional order of the molecules.

Bar graphs are also presented for all of the compounds in this study, **5a–d** and **9a–d**, to get a better view of the odd–even effect. Fig. 2, at the top, represents the melting points for **5a–d** and the transition temperatures upon heating for **9a–d**. At the bottom of Fig. 2, plots of the entropy values for Cr → I for **5a–b** and Cr → N for **9a–d** ($\Delta S/R$) are shown.

Theoretical calculations

Theoretical calculations were performed to evaluate the influence of the number of methylene carbon atoms in the flexible spacer chain on the most stable conformation of the compounds of the series **5a–d**. DFT calculations were carried out in order to obtain the optimized geometries and conformational distributions for the molecules **5a–d**. All of the calculations were performed with the Gaussian 03²⁸ computational package and the geometries were optimized under vacuum using the B3LYP²⁹ hybrid functional with the level 6-311G(d,p) basis set. In order to compare the energies, geometries and dipoles moments with the ones obtained in the gas phase, the structure of **5a** was calculated using the PCM model for the solvent effect and water and cyclohexane as solvents with high and low dielectric constants, respectively.³⁰ Calculations were performed considering that the molecular shape has a prominent effect in liquid crystal behavior and is primarily determined by the rotational process.³¹ The study here is guided by the fact that **5a–d** and **9a–d** containing a five-membered heterocyclic ring, named Δ^2 -isoxazolines, are connected to a benzoate moiety core by a flexible aliphatic spacer. The spacers in liquid crystal dimers contribute to the molecular anisotropy and exert control over the relative orientation of the two mesogenic groups.

The Δ^2 -isoxazolines present a non-traditional bent-shape as a consequence of the tetrahedral carbon atoms C_4 and C_5 in the heterocyclic ring. Deviations from linearity as well as the non-coplanarity of the aryl groups bonded to C_3 and C_5 of isoxazoline have a pronounced influence on the mesophase formation as well as on the liquid crystal mesophase stability. To compensate these geometrical constraints, the elongating molecular strategy is applied for. Previous results have shown that stable mesophase formation is reached when highly anisotropic groups are linked to the C_3 and C_5 isoxazoline carbon atoms.²⁴

For mesogens composed of flexible molecules a large number of conformational states can be obtained due to being arranged antiparallel or inclined for odd and even dimers and degrees of freedom related to the alkyl chains. In fact, calculations performed in this work showed a set of lowest energy conformations for **5a–d** with energy barriers lower than $1.0 \text{ kcal mol}^{-1}$ in the gas phase as well as in the condensed phase.

Fig. 3 represents the lowest energy conformations obtained for **5a–d**. It is interesting to notice that the favored geometry for **5a** is slightly different to **5c** and quite different to **5b** and **5d** because of the dihedral angle ϕ_1 . For **5a**, the dihedral angle ϕ_1 is related to the $O_1-C_5-C_6-O_2$ atoms, whereas for **5b–d** the dihedral angle ϕ_1 is defined between the $C_4-C_5-C_6-C_7$ carbon atoms. In this way, the *antiperiplanar* arrangement of the carbon skeleton of the flexible spacer is obtained with different atoms as the length of spacer increases. Upon increasing from 1 to 4 methylene units in the flexible spacer the preferred rotamers are those that contain all of the methylene units in a *trans* conformation, except for **5a**. **5a** prefers a conformation where the two polar

bonds O_1-C_5 and C_6-O_2 are oriented at an angle of 173.3° to minimize the electrostatic repulsion that occurs in the *gauche* rotamer, where the ϕ_1 angle is equal to 61.8° .

This conformational preference for **5a** can be explained by a destabilizing interaction that occurs when the O_1-C_5 bond of the heterocyclic ring and C_6-O_2 of the ester group are in the *gauche* position. In the *gauche* arrangement (inset at the top of Fig. 3), despite O_1 being on the opposite side to the carbonyl oxygen O_3 , O_1 and O_2 are closer than in the *anti* conformation. To avoid this unfavorable electrostatic repulsion, **5a** shows a more bent-shape form where the O_2 and O_1 oxygen atoms have adopted an *antiperiplanar* disposition. However when the size of the flexible spacer increases through the addition of methylene carbon atoms, this destabilization is no longer observed and now it is its preference for all *trans* conformations for the flexible spacers which is prevailing.

This preference can be explained by minimization of the destabilizing electrostatic interaction created by the *gauche* conformations, thus avoiding the *syn*-pentane effect. A destabilizing *syn*-pentane interaction is created when a hydrocarbon chain is folded such that a g^+ dihedral angle is followed by one g^- along the backbone.³² This effect, primarily of steric origin, results in conformers substantially higher in energy and, for this reason, linear hydrocarbon chains in alkanes adopt conformations that are free of *syn*-pentane interactions.³³ This effect can be clearly seen in the even-numbered members **5b** and **5d**, and the odd-numbered member **5c**.

Statistically, there are a lot of rotamers that contribute to the equilibrium of **5a–d** because of the great number of internal

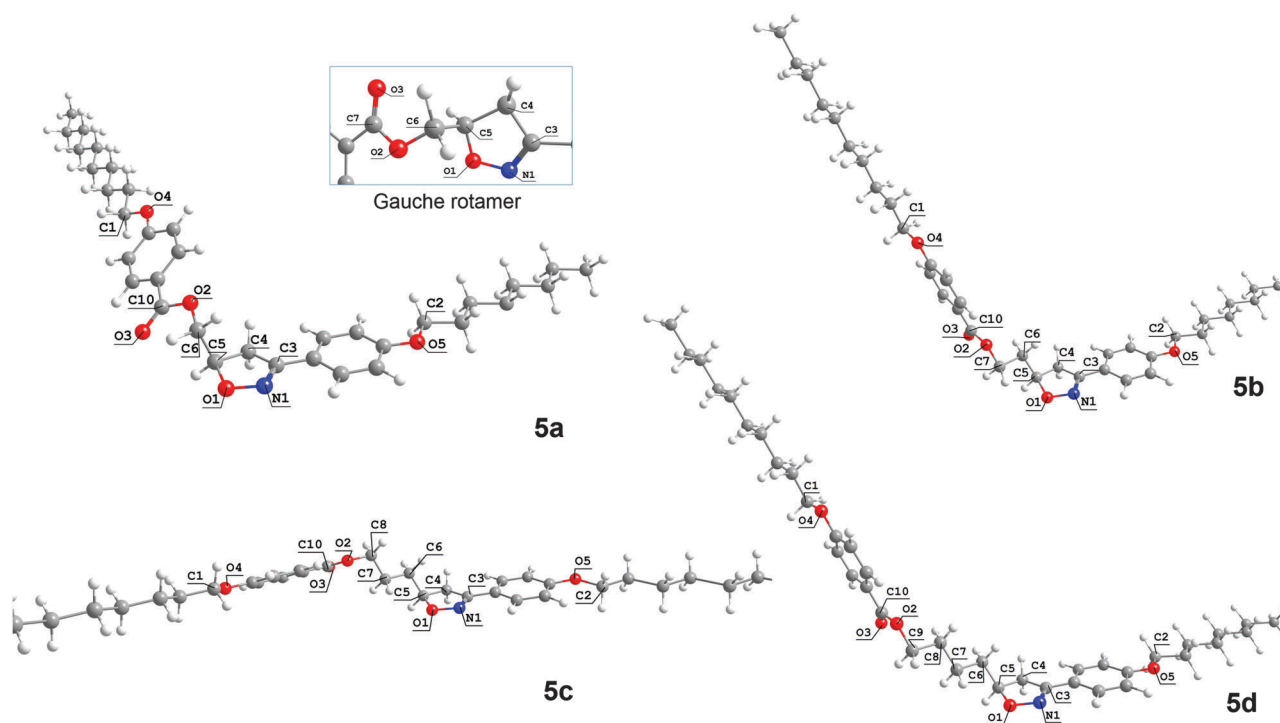


Fig. 3 The most stable **5a–d** molecular structures calculated at the B3LYP/6-311G(d,p) level, in the gas phase. For **5a**, the *gauche* rotamer is shown in the inset at the top and the *anti* rotamer (the most stable) is shown below. **5b–d** all showed the *trans* conformation for the flexible spacer.

degrees of freedom for these molecules. For **5a**, considering the terminal alkyl chains are all *trans*, there are two conformations with a small energy difference between them. One of them is more elongated (the *gauche* conformer) and the other, the most stable, is more bent-shaped and less elongated (the *anti* rotamer in Fig. 3 – **5a**). The energy barrier to convert the most stable rotamer obtained for **5a** into the *gauche* rotamer is 0.67 kcal mol⁻¹. The molecular length of the *gauche* rotamer is 34.8 Å which is about 6 Å bigger than the *anti* rotamer. We can overlook the contribution of all of the conformers to the equilibrium if we restrict the conformers to a discrete number such as the *anti* and *gauche* conformers.³⁴ In doing so the populations in the equilibrium are roughly estimated to be in favor of the more bent-shaped conformer (*anti*) than the less bent-shaped conformer (*gauche*).

The relative orientation of the two molecular planes depends on the conformation of the flexible spacer (see Fig. S33, ESI†). The most stable conformer of **5a** presents two slightly collinear and twisted planes composed of the aromatic rings, isoxazoline ring and terminal alkyl chains. The estimated angle between these two planes is about 32.5° from the side view (see the ESI†). **5c** has similar planes which are shifted by about 60° when compared to the planes of **5a**. These two planes are now separated by 21.5° from the side view. Individually, each rotamer of **5a** has two independent planes which are organized in an edge-to-edge manner. From the top view it is possible to see that the planes are nearly flattened to the normal. For the even-numbered members **5b** and **5d** these planes are bent. The rotamers of **5b** and **5d** are organized in a face-to-face manner with an estimated angle between the planes of 98.5° and 102° for **5b** and **5d**, respectively. The top view of these planes shows that they are tilted to the normal.

Table 2 shows the data for the most stable conformations of **5a–d**. The dipole moments, molecular lengths and some dihedral angles obtained for the *anti* conformation of **5a** in the gas phase, in water and cyclohexane are shown. For **5b–d** the data were collected only in the gas phase. Both the gas phase and condensed phase calculations for **5a** pointed to same conformation as being the most stable conformer, but when solvent effects were taken into account the dipole moment increases with the increase of the solvent dielectric constant.

Table 2 Dipole moments (D), dihedral angles (degrees) and molecular lengths (Å) for **5a–d**. For **5a**, data in water and cyclohexane are also shown. Molecular lengths are measured from carbon to carbon

Entry	μ (Debye)	Dihedral angle, ϕ_1 (°)	Dihedral angle, ϕ_2^e (°)	Dihedral angle, ϕ_3^f (°)	Molecular length (Å)
5a	7.7	173.3 ^c	179.4	176.5	28.96
5a^a	8.5	174.7 ^c	176.2	176.9	29.70
5a^b	9.8	177.0 ^c	175.1	176.8	29.80
5b	5.4	175.6 ^d	179.8	178.0	33.25
5c	3.0	176.7 ^d	0.660	0.86	36.93
5d	5.0	176.9 ^d	176.5	178.6	37.45

^a Cyclohexane. ^b Water. ^c Dihedral angle between the O₁–C₅–C₆–O₂ atoms. ^d Dihedral angle between the C₄–C₅–C₆–C₇ atoms. ^e Dihedral angle N₁–C₃–O₅–C₂. ^f Dihedral angle O₂–C₁₀–O₄–C₁.

The values of dihedral angles ϕ_2 , defined by N₁–C₃ and O₅–C₂, and ϕ_3 , defined by O₂–C₁₀–O₄–C₁, ensure that the alkyl chains and aromatic rings are in the same molecular plane on each side of the molecules. The aliphatic side chains all have *trans* conformations. The carbonyl oxygen, O₃, is always on the opposite side to the O₁–N₁ polar bond of the isoxazoline ring, except for **5a**. In this structure, the carbonyl oxygen is on the same side of the O₁–N₁ polar bond as a consequence of the *antiperiplanar* arrangement.

The main feature of this conformational analysis is related to changes in the dihedral angle related to the flexible spacer (ϕ_1). The ϕ_2 and ϕ_3 dihedral angles are about 180.0° for **5a**, **5b**, and **5d** and about 0° for **5c**. Thus, the **5a**, **5b**, and **5d** molecules display an *antiperiplanar* orientation of the imine group (C=N) and O₅–C₂ bonds. The same *antiperiplanar* orientation is observed for the acyl linkage (OC₁₀–O₂) and O₄–C₁ bonds. A *synperiplanar* orientation was observed for the dihedral angles ϕ_2 and ϕ_3 for **5c** only. This is reflected in a lowering of the dipole moment shown by this molecule.

Theoretical calculations are a powerful tool that helps us to understand the observed dependence of the thermal behavior on the length and the parity of the spacer for **5a–d** and **9a–d**, and even for **7a–d** which are definitely not liquid crystals.³⁵ The even–odd effect of the melting point, and less visibly the enthalpy and entropy changes as the length of the spacer increases, can be explained by the shape of the molecules when considering the conformational issues of the flexible spacer.³⁶ Despite the small differences in the energy barriers for the conformers observed in this study it is possible to assume that the conformers shown in Fig. 3 are at least responsible for the observation of the odd–even effects or partially responsible for the observed behavior. We are assuming that, for example, compounds that have one and three carbon atoms in the flexible spacer (odd-numbered members) are more anisotropic in their V-shape than the even-numbered members, and therefore their enthalpy and entropy values are higher than the even-numbered members.³⁷ Under these circumstances, the melting points of the odd-numbered members are higher than the even-numbered members for all of the compounds listed in Table 1 as a consequence of the better packing for the odd-numbered members. We consider that the molecular packing for the odd-numbered members in an intermolecular V-fashion is face to face where the two molecular planes are nearly flattened to the normal. Even-numbered members may be packed one by one in V-fashion similar to a chevron structure (see Fig. S44, ESI†) considering that the planes are tilted to normal. So the odd-numbered members in this study can absorb more energy without causing disintegration of the crystal lattice until the melting point is reached.

The dependence of the transitional properties of LCs **5a–d** and **9a–d** in relation to the flexible spacer is better seen when observing the melting point. The irregular behavior of the meso-phase makes the analysis more complex due to the enantiotropic or monotropic behavior observed for these LCs (Table 1). The enthalpy values also show a similar effect being more pronounced for the **5a–d** series. The entropy values follow the same tendency

as observed for compounds **5a–d** and **9a–d**. However, the values for **5a–d** are higher due to transitions occurring from the ordered crystalline state to the directly disordered liquid state. LCs which have an enantiotropic mesophase such as **9a** or **9c** have an enhanced anisotropic-shape which allows molecules to pack more efficiently in the mesophase resulting in higher transition temperatures and entropy changes.² It is possible to associate to these LCs the synergy between the conformational distribution and the orientational order of the nematic phase.³³ The mesomorphic behavior found for **9a–d** in this work is due to the presence of the long aromatic moiety terminally bonded to the isoxazoline ring. However, in some cases such as **5a–d** or **7a–d** the molecular dimensions (length-to-breadth ratio) of the aromatic moiety are not sufficient to overcome the non-coplanarity of the isoxazoline ring and the conformational issues of the flexible spacer. In this situation no mesophase or unstable mesophase (*i.e.*, monotropic behavior) appears.

X-ray experiments

In Fig. 4 we present the X-ray results obtained for compound **5a** through varying the temperature of the sample. The spectra were collected during cooling from the isotropic phase, where a broad halo is observed in the isotropic phase at around $2\theta \approx 20^\circ$, which according to Bragg's law corresponds to a distance of about 4.5 Å. This distance is related to the short length correlations between neighboring molecules. It is worth emphasizing that the SmA and SmC phases are almost indistinguishable from X-ray experiments, where in both cases an intense peak appears in the low angle region as a result of the X-ray beam diffraction by the smectic layers. In this case, the assignment is possible with additional techniques such as polarizing optical microscopy.³⁸

By applying Bragg's law to the position of the first intense peak in the SmC phase at 80 °C it is possible to obtain an interlayer spacing of 28.3 Å, as well as, the second ordered peak at 14.6 Å. The ratio of $d_{001}/d_{002} \approx 2$ confirms the smectic

character of the phase. The calculated molecular length (L) for compound **5a** in the lower energetic conformation between the external H atoms is 29.95 Å. Considering that the molecules adopt the most extended form of the aliphatic chains in the mesophase, the tilt angle (θ) of the molecules in the SmC phase can be determined using the expression $\theta = \cos^{-1}(d_{001}/L) = 19$ degrees. Despite the fact that this value is relatively low, the same has been previously obtained for another SmC compound.³⁶ The inset in Fig. 4 shows a schematic representation of the molecular packing according to the optimized molecular structure obtained from the theoretical analysis. Below the SmC–Cr transition temperature at 70 °C, additional peaks appear at the high angle region between 15 and 27 degrees, which are characteristic of the sample crystallization. However, in the low angle region an intense peak is still observed with an associated distance of 22.8 Å. It suggests that the smectic order is preserved, where the reduction of the interlayer distance compared to the one in the SmC phase can be associated to an increase of the tilt angle, to a reduction of the molecular length, or both.

For compound **5b** it was not possible to obtain a clear spectrum of the SmC phase, where the crystallization and the mesophase occur simultaneously for the sample, which was observed right below the isotropic transition. This was due to the narrow temperature region of the SmC phase, but it was also an indication that the SmC phase is very unstable.

Conclusion

Two new series of non-symmetric liquid-crystalline dimers with 3,5-disubstituted 4,5-dihydroisoxazole benzoates and non symmetric isoxazoline derivatives, **5a–d** and **9a–d**, have been synthesized. **5a** and **5b** displayed a monotropic SmC phase whereas **9a–d** displayed an enantiotropic nematic phase for **9a** and **9c**. Monotropic behaviour was observed for **9b** and **9d**. The mesomorphic behavior observed for **9a–d** in this work is due to the presence of the naphthyl aromatic moiety laterally bonded to the isoxazoline ring. A dependence of the melting point thermal behavior on the length and the parity of the spacer was observed for **5a–d** and **9a–d**, and even to **7a–d** which are not definitely not liquid crystals. Transition temperatures, and enthalpy and entropy values for odd-numbered members were higher than those for even-numbered members, reflecting that they are more shape-anisotropic. Density functional theory calculations were performed to evaluate the conformational issues of the flexible spacers and how these influence the mesomorphic behaviour of the dimers. An *antiperiplanar* arrangement was found for all of the carbon atoms of the flexible spacer including the C₄ carbon atom of the isoxazoline ring, except for **5a**. For **5a**, an *antiperiplanar* arrangement was observed when considering the oxygen atom O₁ of the isoxazoline ring. Otherwise, a less stable *gauche* rotamer for **5a** could be observed taking into account the alignment of the carbon atom of the flexible spacer with the heterocyclic C₄ carbon atom. Compounds that have one and three carbon atoms in the

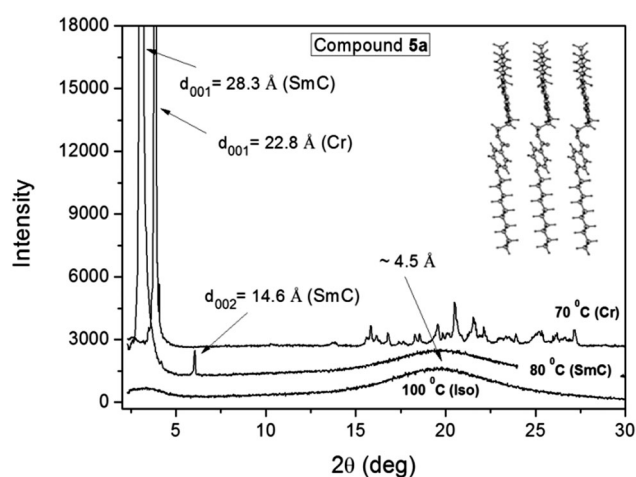


Fig. 4 X-ray spectra of compound **5a** for different temperatures. The inset shows a schematic representation of the molecules in the layered structure.

flexible spacer (odd-numbered members) are more anisotropic in their V-shape than the even-numbered members. Melting points for both of the series **5a-d** and **9a-d** displayed a regular behaviour concerning the length and parity of the flexible spacer. Enthalpy and entropy values for the **5a-d** esters followed the tendency observed for the melting point. However, for **9a-d** the behaviour was irregular, and therefore their enthalpy and entropy values are in general higher than the even-numbered members. Under these circumstances the melting points for the odd-numbered members are higher than the even-numbered members for all of the compounds in this work as a consequence of the better packing of the odd-numbered members.

Acknowledgements

This work was supported by MCT/CNPq, Fapergs-Edital PqG 002/2014. A. A. M. thanks MCT/CNPq for his postdoctoral studies at the University of Hull, Hull, UK (grant no. 201116/2011-1). Thanks to FAPESC, Laboratório de Difração de Raios-X (LDRX-DF/UFSC) for the X-ray diffraction experiments and the Department of Chemistry, University of Hull, Hull, UK for the use of NMR facilities.

References

- C. T. Imrie and G. R. Luckhurst, in *Handbook of Liquid Crystals*, ed. D. Demus, J. Goodby, G. W. Gray, H.-W. Spiess and V. Vill, Wiley-VCH, Weinheim, 1998, vol. 2B, pp. 801–833.
- C. T. Imrie and P. A. Henderson, *Chem. Soc. Rev.*, 2007, **36**, 2096.
- D. Vorlander, *J. Phys. Chem.*, 1927, **126**, 449; D. W. Bruce, K. Heyns and V. Vill, *Liq. Cryst.*, 1997, **23**, 813.
- J. Rault, L. Liebert and L. Strzelecki, *Bull. Soc. Chim. Fr.*, 1975, 1175.
- S. Kumar, *Liq. Cryst.*, 2005, **32**, 1089; J. H. Wild, K. Bartle, N. T. Kirkman, S. M. Kelly, M. O'Neill, T. Stirner and R. P. Tuffin, *Chem. Mater.*, 2005, **17**, 6354; H. Wang, B. Bai, P. Zhang, B. Long, W. Tian and M. Li, *Liq. Cryst.*, 2006, **33**, 445; M. P. Aldred, R. Hudson, S. P. Kitney, P. Vlachos, A. Liedtke, K. L. Woon, M. O'Neill and S. M. Kelly, *Liq. Cryst.*, 2008, **35**, 413.
- B. Kosata, G. M. Tamba, U. Baumeister, K. Pelz, S. Diele, G. Pelzl, G. Galli, S. Samaritani, E. V. Agina, N. I. Boiko, V. P. Shibaev and W. Weissflog, *Chem. Mater.*, 2006, **18**, 691.
- M. G. Tamba, B. Kosata, K. Pelz, S. Diele, G. Pelzl, Z. Vakhovskaya, H. Kresse and W. Weissflog, *Soft Matter*, 2006, **2**, 60.
- I. Sledzinska, E. Bialecka-Florjanczyk and A. Oresko, *Eur. Polym. J.*, 1996, **32**, 1345.
- M. Ibn-Elhaj, A. Skoulios, D. Guillon, J. Newton, P. Hodge and H. J. Coles, *Macromolecules*, 1995, **19**, 1264.
- H. C. Lee, Z. B. Lu, P. A. Henderson, M. F. Achard, W. A. K. Mahmood, G. Y. Yeap and C. T. Imrie, *Liq. Cryst.*, 2012, **39**, 259.
- A. Blumstein and O. Thomas, *Macromolecules*, 1982, **15**, 1264.
- C. V. Yelamagad, I. S. Shashikala and Q. Li, *Chem. Mater.*, 2007, **19**, 6561.
- I. Nishiyama, J. Yamamoto, J. W. Goodby and H. Yokoyama, *J. Mater. Chem.*, 2003, **13**, 2429.
- C. V. Yelamagad, U. S. Hiremath, D. S. S. Rao and S. K. Prasad, *Chem. Commun.*, 2000, 57; A. S. Achalkumar, D. S. S. Rao and C. V. Yelamagad, *New J. Chem.*, 2014, **38**, 4235.
- T. Donaldson, P. A. Henderson, M. F. Achard and C. T. Imrie, *J. Mater. Chem.*, 2011, **21**, 10935.
- C. V. Yelamagad, U. S. Hiremath, D. S. S. Rao and S. K. Prasad, *Chem. Commun.*, 2000, 57.
- A. C. Griffin and T. R. Britt, *J. Am. Chem. Soc.*, 1981, **103**, 4957.
- C. K. Ober, J. I. Jin and R. W. Lenz, *Adv. Polym. Sci.*, 1984, **59**, 103.
- A. Ferrarini, C. Greco and G. R. Luckhurst, *J. Mater. Chem.*, 2007, **17**, 1039.
- H. Wang, R. Shao, C. Zhu, B. Bai, C. Gong, P. Zhang, F. Li, M. Li and N. A. Clark, *Liq. Cryst.*, 2008, **35**, 967.
- R. M. Srivastava, R. A. W. N. Filho, R. Schneider, A. A. Vieira and H. Gallardo, *Liq. Cryst.*, 2008, **35**, 737; B. L. Bai, H. T. Wang, X. L. Lin, X. Ran, C. X. Zhao and M. Li, *Lett. Org. Chem.*, 2012, **9**, 76.
- M. J. Wallage and C. T. Imrie, *J. Mater. Chem.*, 1997, **7**, 1163.
- V. Bezborodov, N. Kauhanka and V. Lapanik, *Mol. Cryst. Liq. Cryst.*, 2004, **411**, 103; V. N. Kovganko and N. N. Kovganko, *Russ. J. Org. Chem.*, 2006, **42**, 696; O. M. S. Ritter, F. C. Giacomelli, J. A. Passo, N. P. Silveira and A. A. Merlo, *Polym. Bull.*, 2006, **56**, 549; J. A. Passo, G. D. Vilela, P. H. Schneider, O. M. S. Ritter and A. A. Merlo, *Liq. Cryst.*, 2008, **35**, 833.
- A. Tavares, P. H. Schneider and A. A. Merlo, *Eur. J. Org. Chem.*, 2009, 889; A. Tavares, P. R. Livotto, P. F. B. Goncalves and A. A. Merlo, *J. Braz. Chem. Soc.*, 2009, **9**, 1742.
- M. A. Weidner-Wells, S. A. Fraga-Spano and I. J. Turchi, *J. Org. Chem.*, 2010, **63**, 6319.
- F. A. Carey and R. J. Sundberg, *Advanced Organic Chemistry, Part B: Reactions and Synthesis*, Plenum Press, 2008; R. Huisgen, in *1,3-Dipolar Cycloaddition Chemistry*, ed. A. Padwa, Wiley, New York, 1984, vol. 1; C. Nájera, J. M. Sansano and M. Yus, *J. Braz. Chem. Soc.*, 2010, **21**, 377.
- U. B. Vasconcelos and A. A. Merlo, *Synthesis*, 2006, 1141.
- M. J. Frisch, G. W. Trucks, H. B. Schlegel, G. E. Scuseria, M. A. Robb, J. R. Cheeseman, J. A. Montgomery Jr., T. Vreven, K. N. Kudin, J. C. Burant, J. M. Millam, S. S. Iyengar, J. Tomasi, V. Barone, B. Mennucci, M. Cossi, G. Scalmani, N. Rega, G. A. Petersson, H. Nakatsuji, M. Hada, M. Ehara, K. Toyota, R. Fukuda, J. Hasegawa, M. Ishida, T. Nakajima, Y. Honda, O. Kitao, H. Nakai, M. Klene, X. Li, J. E. Knox, H. P. Hratchian, J. B. Cross, V. Bakken, C. Adamo, J. Jaramillo, R. Gomperts, R. E. Stratmann, O. Yazyev, A. J. Austin, R. Cammi, C. Pomelli, J. W. Ochterski, P. Y. Ayala, K. Morokuma, G. A. Voth, P. Salvador, J. J. Dannenberg, V. G. Zakrzewski, S. Dapprich, A. D. Daniels, M. C. Strain,

- O. Farkas, D. K. Malick, A. D. Rabuck, K. Raghavachari, J. B. Foresman, J. V. Ortiz, Q. Cui, A. G. Baboul, S. Clifford, J. Cioslowski, B. B. Stefanov, G. Liu, A. Liashenko, P. Piskorz, I. Komaromi, R. L. Martin, D. J. Fox, T. Keith, M. A. Al-Laham, C. Y. Peng, A. Nanayakkara, M. Challacombe, P. M. W. Gill, B. Johnson, W. Chen, M. W. Wong, C. Gonzalez and J. A. Pople, *Gaussian 03, Revision A.1*, Gaussian, Inc., Wallingford CT, 2003.
- 29 A. D. Becke, *J. Chem. Phys.*, 1993, **98**, 5648; C. Lee, W. Yang and R. G. Parr, *Phys. Rev. B: Condens. Matter Mater. Phys.*, 1988, **37**, 785.
- 30 J. Tomasi, B. Mennucci and R. Cammi, *Chem. Rev.*, 2005, **105**, 2999.
- 31 F. A. Carey and R. J. Sundberg, *Advanced Organic Chemistry, Part A*, Plenum Press, New York, 3rd edn, 1990, pp. 117.
- 32 R. W. Hoffmann, *Angew. Chem., Int. Ed.*, 2000, **39**, 2054.
- 33 J. B. Klauda, R. W. Pastor and B. R. Brooks, *J. Phys. Chem. B*, 2005, **109**, 15684.
- 34 P. J. Flory, *Statistical Physics of Chain Molecules*, Wiley, New York, 1969.
- 35 Unfortunately we were not able to get a single crystal of **5a-d** or **9a-d** to be analyzed using X-ray experiments and compare to our DFT studies.
- 36 D. Demus, J. Goodby, G. W. Gray, H. W. Spiess and V. Vill, *Handbook of Liquid Crystals*, Wiley-VCH, Weinheim, New York, Chichester, Brisbane, Singapore, Toronto, 1998, p. 72.
- 37 D. P. Pink, *J. Chem. Phys.*, 1975, **63**, 2533; T. Carnelley, *Philos. Mag.*, 1882, **13**, 112.
- 38 H. Gallardo, F. R. Bryk, A. A. Vieira, T. E. Frizon, G. Conte, B. S. Souza, J. Eccher and I. H. Bechtold, *Liq. Cryst.*, 2009, **36**, 839.